HHS Public Access

Author manuscript

Mol Pharm. Author manuscript; available in PMC 2019 August 06.

Published in final edited form as:

Mol Pharm. 2018 August 06; 15(8): 3434–3441. doi:10.1021/acs.molpharmaceut.8b00424.

ImmunoPET of CD146 in a Murine Hindlimb Ischemia Model

Carolina A. Ferreira[1,‡], **Reinier Hernandez**[2,‡], **Yunan Yang**[2], **Hector F. Valdovinos**[3], **Jonathan W. Engle**[3], and **Weibo Cai**[1,2,3,4,*]

[1]Department of Biomedical Engineering, University of Wisconsin-Madison, Madison, Wisconsin

[2]Department of Radiology, University of Wisconsin-Madison, Madison, Wisconsin

[3]Department of Medical Physics, University of Wisconsin-Madison, Madison, Wisconsin

[4]University of Wisconsin Carbone Cancer Center, Madison, Wisconsin

Abstract

Peripheral Arterial Disease (PAD) consists of a persistent obstruction of lower-extremity arteries further from the aortic bifurcation attributable to atherosclerosis. PAD is correlated with an elevated risk of morbidity and mortality as well as of deterioration of the quality of life with claudication and chronic leg ischemia being the most frequent complications. Therapeutic angiogenesis is a promising therapeutic strategy that aims to restore the blood flow to the ischemic limb. In this context, assessing the efficacy of pro-angiogenic treatment using a reliable non-invasive imaging technique would greatly benefit the implementation of this therapeutic approach. Herein, we describe the angiogenesis and perfusion recovery characteristics of a mouse model of PAD *via in vivo* positron emission tomography (PET) imaging of CD146 expression. For that, ischemia was generated by ligation and excision of the right femoral artery of Balb/C mice and confirmed through Laser Doppler imaging. The angiogenic process, induced by ischemia, was non-invasively monitored and quantified through PET imaging of CD146 expression in the injured leg using a ^{64}Cu-labeled anti-CD146 monoclonal antibody, ^{64}Cu-NOTA-YY146, at postoperative days 3, 10 and 17. The CD146-specific character of ^{64}Cu-NOTA-YY146 was verified *via* a blocking study performed in another cohort at day 10 after surgery. Tracer uptake was correlated with *in situ* CD146 expression by histological analysis. PET scans results indicated that ^{64}Cu-NOTA-YY146 uptake in the injured leg was significantly higher, with a highest uptake with a value of 14.1 ± 2.0 %ID/g at postoperative day 3, compared to the normal contralateral hindlimb, at all time points (maximum uptake of 2.2 ± 0.2 %ID/g). The pre-injection of a blocking dose resulted in a significantly lower tracer uptake in the ischemic hindlimb on day 10 after surgery, confirming tracer specificity. CD146/CD31 immunofluorescent co-staining showed excellent correlation between the high uptake of the tracer with *in situ* CD146 expression levels and a marked co-localization of CD146 and CD31 signals. In conclusion, persistent and CD146-specific tracer accumulation in the ischemic hindlimb was observed, confirming the feasibility of ^{64}Cu-

*Corresponding Author: Weibo Cai, PhD. Address: Department of Radiology, University of Wisconsin - Madison, Room 7137, 1111 Highland Avenue, Madison, WI 53705, USA. wcai@uwhealth.org; Phone: 608-262-1749; Fax: 608-265-0614.
‡These authors contributed equally.

Author Contributions

The manuscript was written through contributions of all authors. All authors have given approval to the final version of the manuscript.

CONFLICT OF INTEREST: The authors declare that they have no conflict of interest.

NOTA-YY146 to be used as an imaging agent to monitor the progression of angiogenesis and recovery in future PAD research.

Graphical Abstract

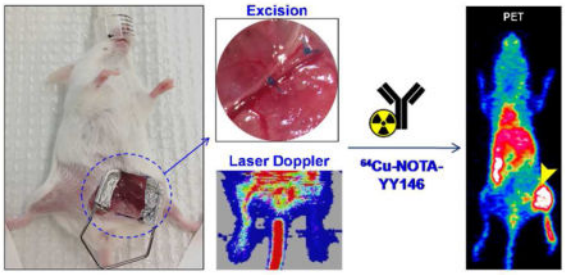

Keywords

positron emission tomography (PET); ^{64}Cu; CD146; hindlimb ischemia; angiogenesis; peripheral artery disease (PAD)

INTRODUCTION

One in three U.S. adults has at least one type of cardiovascular disease (CVD)[1]. Peripheral arterial disease (PAD) is one of the manifestations of CVD that affects an estimate of 12–20% Americans over 65 years of age and accounts for a major portion of CVD-related morbidity and mortality[2,3]. PAD significantly decreases quality of life, results in a progressive decay in function of the lower extremities over time[4,5], and have shown to triple the 5-year mortality rate in patients with intermittent claudication[6]. PAD is an atherosclerotic process that causes stenosis and occlusion of peripheral arteries, resulting in tissue hypoxia[7]. Ischemic tissues are known to secrete paracrine angiogenic factors, especially vascular endothelial growth factor (VEGF) and others, that subsequently induce angiogenesis as a compensatory response to reestabilsh the blood circulation[8].

Therapeutic angiogenesis, which is the stimulation of growth of new blood vessels to replace diseased and dysfunctional arteries, represents an auspicious approach that could restore peripheral circulation and quality of life in PAD patients. For that reason, PAD patients are always considered for revascularization therapies with the goals of relieving pain, healing ischemic ulcers and preventing limb loss[9]. Growth factors and other several pro-angiogenic treatments have been suggested to improve tissue revascularization in PAD[10,11]. In this sense, *in vivo* visualization of angiogenic reperfusion can potentially be a fundamental approach to ascertain PAD development, monitoring and response to treatment. However, evaluation of proangiogenic-based therapies has been limited by the lack of reliable, non-invasive imaging methods[12].

Conventional imaging approaches such as Doppler ultrasonography, magnetic resonance imaging (MRI), and contrast angiography are generally used to investigate ischemic process in PAD patients[8,13], but each has its disadvantages such as low reproducibility, inability to

provide precise information on subtle changes in blood flow, and low sensitivity for molecularly targeted imaging[14,15]. In contrast, Positron emission tomography (PET), is a noninvasive quantitative molecular imaging technique that can provide a sensitive evaluation of the processes that regulate vascular disease pathogenesis, progression, and therapeutic response, including the assessment of angiogenesis as a results of limb ischemia[16]. Several radiolabeled imaging agents designed to monitor PAD-induced angiogenesis have been described, mostly based on antibodies that target VEGF receptors or small molecules targeting integrin receptors[17]. CD146 (cluster of differentiation 146) is a cell adhesion molecule (CAM) that has been identified as a marker of vascular endothelial cells; it is highly expressed on the entire vascular tree during embryogenesis, and crucially participates in vascular development thereafter. Moreover, CD146 expression have shown to drive, in part, tumor-angiogenesis in several types of tumors, supporting evidence that CD146 is a feasible marker for angiogenesis[18]. Our group has previously described the development of a CD146-targeting tracer through radiolabeling of YY146, a murine anti-CD146 monoclonal antibody, for successful immunoPET imaging of a diverse range of murine tumor models overexpressing CD146[19–22].

Herein, we report the use of ^{64}Cu-NOTA-YY146 (NOTA denotes 1,4,7-triazacyclononane-1,4,7-triacetic acid) for the quantitative, non-invasive monitoring of angiogenesis in a murine hindlimb ischemia model of PAD through PET imaging. The mouse hindlimb ischemia is a well-established model that provides a well-defined and previously-characterized platform that is integral to preclinical studies both for testing new therapeutic angiogenesis strategies and for studying the mechanistic control of neovascularization *in vivo*[23]. CD146 expression levels in that model were non-invasively assessed for up to 2 weeks and validated by PET imaging, Laser Doppler imaging, biodistribution data and immunohistochemical analysis.

EXPERIMENTAL SECTION

Mouse model of hindlimb ischemia

All animal studies were conducted under a protocol approved by the University of Wisconsin Institutional Animal Care and Use Committee. A thorough protocol of induction of unilateral hindlimb ischemia have been described elsewhere[24,25]. Briefly, six-week-old female BALB/c mice (Envigo, Madison, WI) were anestesized and hindlimb ischemia in the right leg was induced through a roughly 3 step process: (i) exposition of the femoral triangle, (ii) isolation followed by occlusion of proximal and distal ends of the femoral artery proximal to the popliteal artery and finally (iii) excision of the transect segment of femoral artery between the suture knots. An internal control was done by performing a sham procedure on the contralateral leg. Since wound healing is naturally a highly angiogenic process, the incision was located on the mid-abdominal level to exclude the likelihood of superposition of radioactivity signals from the ischemic muscle tissue and the surgical wound.

NOTA Conjugation and ^{64}Cu-labeling of YY146

Comprehensive procedure details for NOTA conjugation, ^{64}Cu production and labeling have been previously reported[22]. In brief, p-SCN-Bn-NOTA in DMSO was added to an antibody solution (approximately 3mg of YY146 in PBS), in a 5:1 molar ratio; pH was adjusted to 8.5–9.0 with Na_2CO_3 (0.1 M) and the reaction was kept shaking at room temperature for 2h. The conjugated antibody was purified through a size exclusion PD-10 column (GE Healthcare) with PBS (pH 7.0) as the mobile phase. 50–100μg of NOTA-YY146 was then added to 74-148MBq (2–4mCi) of $^{64}CuCl_2$ in 300 μL of NaAc buffer (0.1 M, pH 4.5) and kept shaking (500 rpm) at body temperature (37 °C) for 30 min. ^{64}Cu-NOTA-YY146 was separated from free ^{64}Cu also using PD-10 columns. Radio-instant thin-layer chromatography (iTLC), with EDTA 50mM (pH 4.5) as mobile phase, was used to assess the labeling yields and radiochemical purity of the radiolabeled compound.

Small animal PET Imaging and biodistribution studies

An Inveon microPET/micro-CT rodent model scanner (Siemens Medical Solutions) was used to obtain PET Scans. For that, the animals (n=4) were tail-vein injected with 5–10 MBq (135–270μCi) of ^{64}Cu-NOTA-YY146 and anesthetized with isoflurane (4% for induction and 2% for maintenance). PET scans were recorded in similar conditions to previously reported[12] at 4, 24, and 48 h after the injection of ^{64}Cu-NOTA-YY146. A total of three longitudinal PET studies were performed at days 3, 10 and 17 after the hindlimb ischemia generation surgery. To assess the ^{64}Cu-NOTA-YY146 specificity *in vivo*, a receptor-blocking study (n=3) was carried out in which the animals were first injected with a blocking dose (10 mg/kg) of unlabeled YY146 24 hours prior to the administration of the radiolabeled antibody. Images were obtained following the same protocol described above and analyzed accordingly. Inveon Research Workplace software (Siemens Medical Solutions) was used to perform region-of-interest (ROI) analysis and quantify tracer uptake in major tissues. Quantitative results are given as percentage injected dose per gram of tissue (%ID/g; mean ± SD).

Also at postoperative days 3, 10 and 17, a separate group of mice were administered intravenously 3.7 MBq (100 μCi) of ^{18}F-FDG and then kept under isoflurane anesthesia for an uptake period of 1h. Images were acquired using the same protocol described for small animal PET imaging studies and analyzed accordingly.

Ex vivo biodistribution studies were carried out to validate the veracity of PET findings as well as to obtain a full biodistribution profile of the ^{64}Cu-NOTA-YY146. Promptly after the final PET scan at 48 h p.i., on postoperative day 17, mice were euthanized by CO_2 asphyxiation, and all major organ/tissues as well as blood were collected and weighed. The radioactivity of each tissue was measured using a WIZARD2 automated gamma-counter (Perkin-Elmer). Quantified tissue uptake is herein reported as %ID/g (mean ± SD).

Laser Doppler Imaging of hindlimb perfusion

Laser Doppler images were acquired before and immeditaly upon surgery as well as at postoperative days 3, 10 and 17 using a laser Doppler imaging system (moorLDI2-HR,

Moor Instruments, DE, USA). During the procedure, the core temperature of the animals was monitored to ensure euthermia.

Histology

Muscular tissue from the operated hindlimb was harvested, at different timepoints, and frozen in Tissue-Tek O.C.T compound (Sakura Finetek U.S.A., Inc. CA). The slices were fixed as reported previously[12] and then incubated with a mixture of YY146 (5 μg/mL) and rat anti-mouse CD31 antibody (BD Biosciences, San Jose, CA) for 1 h at RT. To allow visualization of positive areas, the slices were then incubated with AlexaFluor488-labeled goat anti-human IgG (Invitrogen, Eugene, OR) and Cy3-labeled donkey anti-rat IgG (Jackson Laboratories, West Grove, PA) secondary antibodies. All images were acquired with a Nikon Eclipse Ti-E microscope.

Statistical analysis

Data are presented as mean ± standard deviation (SD). The 2-tailed paired and unpaired Student *t*-tests were used to test differences within animals (ischemic versus non-ischemic contralateral hindlimb of mice) and between animals of different groups. A P value less than 0.05 was considered statistically significant. The authors had full access to and took full responsibility for the integrity of the data.

RESULTS

Laser Doppler Imaging of hindlimb perfusion

Hindlimb ischemia was generated in the right leg through excision of the right femoral artery, with clear diminished blood flow in the right leg post-ischemia (Figure 1), confirmed by laser Doppler imaging. Since our group have already successfully used this hindlimb ischemia model in a quantitative manner[12,26] and have demonstrated that the average injured tissue perfusion ratio decreased from 0.896 ± 0.098 right before surgery to 0.218 ± 0.077 right after surgery ($n = 3$; $P < 0.01$)[12], and that, by day 17, the perfusion ratio was 0.81 ± 0.24[26], herein we present Laser Doppler Imaging more qualitatively to analyze blood perfusion. It is possible to observe (Figure 2D) that the blood flow was largely restituted by postoperative day 17, in accordance with previously published studies[12,26].

^{18}F-FDG PET Imaging

Longitudinal ^{18}F-FDG scans were performed to evaluate the status of inflammatory processes in the operated leg on postoperative days 3, 10 and 17 (Figure 2A). ROI analysis of the PET images was used to quantify the ^{18}F-FDG uptake in the heart, liver, kidneys as well as normal and ischemic legs (Figure 2B). The uptake in the heart was above 30% ID/g for all the time points, while the uptake in the kidney was 20.8 ± 1.8, 24.7 ± 8.6 and 14.1 ± 1.9 %ID/g at postoperative days 3, 10 and 17 respectively. The maximum uptake in the liver was found to be 5.5 ± 0.5 % ID/g at day 10. ^{18}F-FDG uptake in the ischemic leg versus normal leg (Figure 2C) was significantly different ($p < 0.05$) at postoperative days 3 and 10, but non-significantly different at day 17. The uptake values for the normal and ischemic leg were 1.1 ± 0.1 vs. 3.1 ± 0.3 %ID/g, 1.8 ± 0.3 vs. 4.9 ± 0.2 %ID/g, and 2.2 ± 0.7 vs. 3.3 ± 0.7 %ID/g at days 3, 10, and 17, respectively.

NOTA Conjugation and ^{64}Cu-labeling of YY146

Radiolabeling of ^{64}Cu-NOTA-YY146 was carried out with high labeling yield (> 80%) with radiochemical purity of > 95%, as both determined by instant thin-layer chromatography. Owning to the high specific activity of $^{64}CuCl_2$ we were able to attain a specific activity for the purified ^{64}Cu-NOTA-YY146 of~185 MBq (5 mCi)/μmol.

^{64}Cu-NOTA-YY146 PET Imaging and biodistribution studies

Mice (n=4) were injected, through the tail vain, with ^{64}Cu-NOTA-YY146 on postoperative days 3, 10 and 17 and longitudinal PET images were acquired at 3, 24 and 48h post-injection. Sequential PET scans are displayed as maximum intensity projections (Fig. 3A). ROI analysis of PET imaging was done to quantify the tracer uptake, represented as %ID/g, in the normal and ischemic legs (Figure 3B and C). At 3 h p.i., a relatively high level of the radiotracer in the blood and a background signal in the abdominal area was found for all postoperative days, attributed to the long circulation half-life of the radiolabeled antibody, in agreement with previous studies in which the accumulation in the tissue of interest peaked in between 24 and 48h p.i[19,27].

Uptake of ^{64}Cu-NOTA-YY146 in the injured hindlimb peaked at 48h p.i., with similar values of 14.1 ± 2.0 and 13.6 ± 0.9 %ID/g on days 3 and 10 after surgery, respectively (n=4; Figure 3B). A notably lower accumulation of the radiotracer, 6.0 ± 0.6 %ID/g at 24h p.i., was observed on postoperative day 17. The maximum ^{64}Cu-NOTA-YY146 accretion in the non-ischemic contralateral hindlimb at 48 h p.i. was consistent throughout the study, 2.2 ± 0.2, 1.9 ± 0.3 and 2.2 ± 0.8 %ID/g on postoperative days 3, 10, and 17, respectively, which were significantly ($p<0.0001$ for days 3 and 10 and $p=0.0012$ for day 17) lower compared to the ischemic hindlimb uptake.

The administration of a blocking dose of the anti-CD146 monoclonal antibody YY146 24h prior to the injection of ^{64}Cu-NOTA-YY146 resulted in a significantly ($p<0.01$) lower tracer uptake in the ischemic leg on day 10 after surgery, with values of 4.8 ± 0.9, 9.3 ± 0.7 and 9.7 ± 1.7 %ID/g at 4, 24 and 48 h p.i., respectively (n = 3; Figure 4B), thus evidencing the CD146 specificity of the tracer *in vivo*. However, at 48h (n = 3, Figure 4C), the uptake in the ischemic leg (9.7± 1.7 %ID/g) was still significantly higher ($p=0.0014$) than that of the non-operated hindlimb (1.7 ± 0.1%ID/g), but still significantly lower ($p<0.05$) to what was observed in the group without blocking (4.2± 0.2, 11.2 ± 0.6 and 13.6 ± 0.9 %ID/g at 4, 24 and 48 h p.i., respectively).

Following terminal *in vivo* PET scans at 48h p.i. on day 17, or day 10 for the blocking study, mice were euthanized, organs were removed, dried on filter paper, and placed in pre-weighed plastic test tubes. The radioactivity was measured using an automatic gamma counter. *Ex vivo* biodistribution studies results correlated well with the obtained PET data and allowed a more thorough characterization of ^{64}Cu-NOTA-YY146's biodistribution as well as the effect of blocking in the tracer uptake (Figure 5A,B). The uptake in the ischemic and non-ischemic legs, with values of 3.5 ± 1.5 and 1.2 ± 0.4 %ID/g respectively, were in agreement with observed with PET imaging. This relatively lower and similar uptake pattern between normal and ischemic leg uptake found at *ex vivo* biodistribution results, at day 17,

is expected since at day 17 after surgery, the injury is repaired, blood flow was already largely restituted and, thus, CD146 expression returned to a normal level. Blood pool radiotracer uptake was found to be 13.1 ± 5.0 %ID/g. Except for liver, lung, kidney, and spleen, with moderate uptakes of 14.2 ± 10.2, 7.4 ± 3.5, 6.9 ± 1.5, 9.1 ± 1.0 %ID/g respectively, non-target tissues showed very low levels of radiotracer uptake. A similar pattern was observed in the mice from the blocking study, in which the uptake values of the ischemic (7.7 ± 3.0 %ID/g) and normal (1.1 ± 0.2 %ID/g) legs were in agreement with findings of PET.

Histology

Ex vivo immunofluorescence CD146 and CD31 staining of ischemic hindlimb muscle sections provided additional information regarding the spatial and temporal distribution of *in situ* CD146 expression following surgery, offering details regarding the vasculature. Representative CD31/CD146 co-staining images are shown in Figure 6. Expression of CD146, shown in the green fluorescence channel, was highest at postoperative day 3, closely followed by day 10. Muscle sections at postoperative day 17 exhibited a reduced fluorescence signal that was comparable to those observed in sections acquired right after surgery. Additionally to CD146, CD31 expression was examined for identification of vasculature. CD31 staining, shown in the red fluorescence channel, co-localized with CD146 staining and presented similar pattern observed with CD146 and was highest at postoperative day 3. These results align well with the findings from *in vivo* and *ex vivo* studies.

DISCUSSION

PAD affects almost 12% of both female and male adult population, with critical limb ischemia (CLI) and claudication being the most common presentation. Approximately 30% of all patients with CLI will have had an amputation and only 45% will be alive with both legs intact within 1 year of the disease. Although the course of treatment varies significantly, some form of revascularization is often used as major therapy[28]. Augmentation of lower-extremity blood flow through vasculogenesis, arteriogenesis or angiogenesis, could be an auspicious tool for improved therapy for patients with PAD. Promising benefits of these treatments include augmented wound healing, lower risk of limb amputation as well as enhanced claudication distance[29]. Several angiogenic therapies have been assessed; however, despite significant evidence of efficacy in preclinical studies, negative results have been found on larger randomized clinical trials. This could be somewhat related to limited knowledge regarding the dose, frequency and method of administration of angiogenic compounds in patients with PAD[30].

In this context, a trustworthy, non-invasive imaging technique to monitor not only the molecular changes during ischemic diseases but also the changes during and after the course of therapeutic regimens, especially angiogenic-based therapies, would be extremely valuable. Molecular imaging methods, including PET, have compelling advantages over conventional vascular imaging techniques (contrast, MR and CT angiographies) and are greatly suited to the visualization and quantification of angiogenic processes for being

tomographic and very sensitive nature[13,26] with superior spatial and temporal resolution and robust attenuation correction.

Nuclear medicine methods for imaging molecular markers of angiogenic process in ischemia models have been deeply explored [13,25,31–34]. Among the most commonly employed radiotracer for imaging of angiogenesis are radiolabeled vascular endothelial growth factor (VEGF) protein and cyclic arginine-glycine-aspartic acid (RGD) peptides. Although those studies show a difference in the uptake between normal and ischemic hindlimb, the ischemic hindlimb muscle uptake typically ranged from around 2%ID/g, which reduces the detection sensitivity of these methods and thus the translational capability of these tracers into the clinical settings. In this study, we conducted non-invasive PET imaging studies of ischemic reperfusion in a hindlimb ischemia model using a monoclonal antibody targeting CD146, which showed an average ischemic hindlimb muscle uptake of approximately 15 %ID/g, a significant increase over previously reported studies. ^{64}Cu-NOTA-YY146 uptake increased to a large extent in the ischemic hindlimb when compared to the non-operated leg and reached the highest level at day 3 post surgery, which correlated well with CD146 expression levels as determined by histological analysis.

The specificity of our tracer was further verified via a blocking study, in which a significant reduction ($p<0.01$) in radiotracer uptake in the operated hindlimb was observed when CD146 receptors were saturated by an injection of a blocking dose (10 mg/kg) of the cold monoclonal antibody. ^{18}F-FDG scans were performed to evaluate the presence of inflammatory processes in the operated leg, which could lead to an increased non-specific ^{64}Cu-NOTA-YY146 accretion. ^{18}F-FDG uptake in the ischemic hindlimb, despite being significantly higher compared to the non-operated leg at postoperative das 3 and 10, was still considered to be very low and the inflammatory status of the operated leg would not significantly affect the overall biodistribution of ^{64}Cu-NOTA-YY146.

Altogether, we have shown that the radiolabeled YY146 successfully fulfilled the purpose of this study. Worth mentioning, our group have previously imaged ischemic-induced angiogenesis using a different monoclonal antibody, anti-CD105, with similar results[12]. Interestingly, CD105 and CD146 take part in different paths of the angiogenic process: CD105 modifies the phosphorylation status of Smad proteins, ultimately regulating TGF-β receptor signaling[35], while CD146 plays essential roles in initial and late stages of angiogenesis promotion and have shown to act as a receptor for netrin-1 in stimulating vascular development[36], as a co-receptor for VEGFR-2 in angiogenesis[37] as well as being involved in the p38/IKK/NF kappaB pathway[38]. Therefore, since CD146 angiogenic behavior is distinct from that of CD105, PET imaging with radiotracers that are distinct for different angiogenesis pathways, such those that allow monitoring of CD146 expression in PAD models, can provide useful complementary information to the existing tracers.

Even though the mouse hindlimb ischemia model provides a well-defined and previously-characterized platform for PAD preclinical studies, in the present study, hindlimb ischemia was generated in healthy balb/c mice. Mouse strain as well as age, presence of atherosclerotic process and/or hypercholesterolemia have shown to affect collateral vessel development and consequently angiogenic markers expression levels [39,40]. For that reason,

we believe that future studies in different animal models that better reflect the vascular status of PAD patients would be valuable. Moreover, the utilization of ^{64}Cu-NOTA-YY146 to monitor drug-mediated angiogenesis as a method to detect changes during ischemic reperfusion is warranted in future studies.

CONCLUSION

The current study described *in vivo* imaging of angiogenic ischemic perfusion recovery through PET using a CD146 targeted monoclonal antibody in a hindlimb ischemia model in mice. ^{64}Cu-NOTA-YY146 presented high *in vivo* CD146-affinity as demonstrated by persistent and CD146-specific uptake in the ischemic hindlimb, thus evidencing its potential to be used as a PET imaging agent. These findings were further validated through several *in vitro, in vivo* and *ex vivo* experiments. Our results warrant further exploration of ^{64}Cu-NOTA-YY146 not only as an imaging tracer in PAD-related research but also in other pathologies in which CD146 expression imaging and monitoring are desired.

Acknowledgments

This work was supported, in part, by the University of Wisconsin – Madison, the National Institutes of Health (P30CA014520 and T32CA009206) and the Brazilian Science without Borders Program (SwB-CNPq). No potential conflict of interest relevant to this article was reported.

References

1. Lloyd-Jones D, Adams RJ, Brown TM, Carnethon M, Dai S, De Simone G, Ferguson TB, Ford E, Furie K, Gillespie C, et al. Heart Disease and Stroke Statistics--2010 Update: A Report from the American Heart Association. Circulation. 2010; 121(7):e46–e215. [PubMed: 20019324]
2. Hirsch AT, Criqui MH, Treat-Jacobson D, Regensteiner JG, Creager MA, Olin JW, Krook SH, Hunninghake DB, Comerota AJ, Walsh ME, et al. Peripheral Arterial Disease Detection, Awareness, and Treatment in Primary Care. JAMA. 2001; 286(11):1317–1324. [PubMed: 11560536]
3. Ostchega Y, Paulose-Ram R, Dillon CF, Gu Q, Hughes JP. Prevalence of Peripheral Arterial Disease and Risk Factors in Persons Aged 60 and Older: Data from the National Health and Nutrition Examination Survey 1999–2004. J Am Geriatr Soc. 2007; 55(4):583–589. [PubMed: 17397438]
4. McDermott MM, Greenland P, Liu K, Guralnik JM, Celic L, Criqui MH, Chan C, Martin GJ, Schneider J, Pearce WH, et al. The Ankle Brachial Index Is Associated with Leg Function and Physical Activity: The Walking and Leg Circulation Study. Ann Intern Med. 2002; 136(12):873–883. [PubMed: 12069561]
5. McDermott MM, Liu K, Greenland P, Guralnik JM, Criqui MH, Chan C, Pearce WH, Schneider JR, Ferrucci L, Celic L, et al. Functional Decline in Peripheral Arterial Disease: Associations with the Ankle Brachial Index and Leg Symptoms. JAMA. 2004; 292(4):453–461. [PubMed: 15280343]
6. Kannel WB, McGee DL. Update on Some Epidemiologic Features of Intermittent Claudication: The Framingham Study. J Am Geriatr Soc. 1985; 33(1):13–18. [PubMed: 3965550]
7. Abdulhannan P, Russell DA, Homer-Vanniasinkam S. Peripheral Arterial Disease: A Literature Review. Br Med Bull. 2012; 104:21–39. [PubMed: 23080419]
8. Clair D, Shah S, Weber J. Current State of Diagnosis and Management of Critical Limb Ischemia. Curr Cardiol Rep. 2012; 14(2):160–170. [PubMed: 22311595]
9. Hess CN, Norgren L, Ansel GM, Capell WH, Fletcher JP, Fowkes FGR, Gottsater A, Hitos K, Jaff MR, Nordanstig J, et al. A Structured Review of Antithrombotic Therapy in Peripheral Artery Disease With a Focus on Revascularization: A TASC (InterSociety Consensus for the Management of Peripheral Artery Disease) Initiative. Circulation. 2017; 135(25):2534–2555. [PubMed: 28630267]

10. Mikroulis D, Papanas N, Maltezos E, Bougioukas G. Angiogenic Growth Factors in the Treatment of Peripheral Arterial Disease. 2007:195–209.
11. Jones WS, Annex BH. Growth Factors for Therapeutic Angiogenesis in Peripheral Arterial Disease. 2007:458–463.
12. Orbay H, Zhang Y, Hong H, Hacker TA, Valdovinos HF, Zagzebski JA, Theuer CP, Barnhart TE, Cai W. Positron Emission Tomography Imaging of Angiogenesis in a Murine Hindlimb Ischemia Model with ^{64}Cu-Labeled TRC105. Mol Pharm. 2013; 10(7):2749–2756. [PubMed: 23738915]
13. Orbay H, Hong H, Zhang Y, Cai W. PET/SPECT Imaging of Hindlimb Ischemia: Focusing on Angiogenesis and Blood Flow. Angiogenesis. 2013; 16(2):279–287. [PubMed: 23117521]
14. Tang GL, Chin J, Kibbe MR. Advances in Diagnostic Imaging for Peripheral Arterial Disease. Expert Rev Cardiovasc Ther. 2010; 8(10):1447–1455. [PubMed: 20936931]
15. Pollak AW, Norton P, Kramer CM. Multimodality Imaging of Lower Extremity Peripheral Arterial Disease: Current Role and Future Directions. Circ Cardiovasc imaging. Nov.2012 :797–807. [PubMed: 23169982]
16. Stacy MR, Maxfield MW, Sinusas AJ. Targeted Molecular Imaging of Angiogenesis in PET and SPECT: A Review. Yale J Biol Med. 2012; 85(1):75–86. [PubMed: 22461745]
17. Haubner R, Beer AJ, Wang H, Chen X. Positron Emission Tomography Tracers for Imaging Angiogenesis. Eur J Nucl Med Mol Imaging. 2010; 37(Suppl 1):S86–103. [PubMed: 20559632]
18. Wang Z, Yan X. CD146, a Multi-Functional Molecule beyond Adhesion. Cancer Lett. 2013; 330(2):150–162. [PubMed: 23266426]
19. Sun H, England CG, Hernandez R, Graves SA, Majewski RL, Kamkaew A, Jiang D, Barnhart TE, Yang Y, Cai W. ImmunoPET for Assessing the Differential Uptake of a CD146-Specific Monoclonal Antibody in Lung Cancer. Eur J Nucl Med Mol Imaging. 2016; 43(12):2169–2179. [PubMed: 27342417]
20. Hernandez R, Sun H, England CG, Valdovinos HF, Barnhart TE, Yang Y, Cai W. ImmunoPET Imaging of CD146 Expression in Malignant Brain Tumors. Mol Pharm. 2016; 13(7):2563–2570. [PubMed: 27280694]
21. Hernandez R, Sun H, England CG, Valdovinos HF, Ehlerding EB, Barnhart TE, Yang Y, Cai W. CD146-Targeted immunoPET and NIRF Imaging of Hepatocellular Carcinoma with a Dual-Labeled Monoclonal Antibody. Theranostics. 2016; 6(11):1918–1933. [PubMed: 27570560]
22. Yang Y, Hernandez R, Rao J, Yin L, Qu Y, Wu J, England CG, Graves SA, Lewis CM, Wang P, et al. Targeting CD146 with a ^{64} Cu-Labeled Antibody Enables in Vivo immunoPET Imaging of High-Grade Gliomas. Proc Natl Acad Sci. 2015; 112(47):E6525–E6534. [PubMed: 26553993]
23. Couffinhal T, Silver M, Zheng LP, Kearney M, Witzenbichler B, Isner JM. Mouse Model of Angiogenesis. Am J Pathol. 1998; 152(6):1667–1679. [PubMed: 9626071]
24. Niiyama H, Huang NF, Rollins MD, Cooke JP. Murine Model of Hindlimb Ischemia. J Vis Exp. 2009
25. Orbay H, Zhang Y, Hong H, Hacker TA, Valdovinos HF, Zagzebski JA, Theuer CP, Barnhart TE, Cai W. Positron Emission Tomography Imaging of Angiogenesis in a Murine Hindlimb Ischemia Model with 64 Cu-Labeled TRC105. Mol Pharm. Jul; 2013 1(107):2749–2756.
26. Orbay H, Hong H, Koch JM, Valdovinos HF, Hacker TA, Theuer CP, Barnhart TE, Cai W. Pravastatin Stimulates Angiogenesis in a Murine Hindlimb Ischemia Model: A Positron Emission Tomography Imaging Study with (64)Cu-NOTA-TRC105. Am J Transl Res. 2013; 6(1):54–63. [PubMed: 24349621]
27. Yang Y, Hernandez R, Rao J, Yin L, Qu Y, Wu J, England CG, Graves SA, Lewis CM, Wang P, et al. Targeting CD146 with a 64Cu-Labeled Antibody Enables in Vivo immunoPET Imaging of High-Grade Gliomas. Proc Natl Acad Sci U S A. 2015; 112(47):E6525–34. [PubMed: 26553993]
28. Fowkes FGR, Aboyans V, Fowkes FJI, McDermott MM, Sampson UKA, Criqui MH. Peripheral Artery Disease: Epidemiology and Global Perspectives. Nat Rev Cardiol. 2016; 14:156. [PubMed: 27853158]
29. Olin JW, White CJ, Armstrong EJ, Kadian-Dodov D, Hiatt WR. Peripheral Artery Disease: Evolving Role of Exercise, Medical Therapy, and Endovascular Options. J Am Coll Cardiol. 2016; 67(11):1338–1357. [PubMed: 26988957]

30. Cooke JP, Losordo DW. Modulating the Vascular Response to Limb Ischemia. Circ Res. 2015; 116(9):1561–1578. [PubMed: 25908729]

31. Hua J, Dobrucki LW, Sadeghi MM, Zhang J, Bourke BN, Cavaliere P, Song J, Chow C, Jahanshad N, van Royen N, et al. Noninvasive Imaging of Angiogenesis with a 99mTc-Labeled Peptide Targeted at alphavbeta3 Integrin after Murine Hindlimb Ischemia. Circulation. 2005; 111(24): 3255–3260. [PubMed: 15956134]

32. Lee K-H, Jung K-H, Song S-H, Kim DH, Lee BC, Sung HJ, Han Y-M, Choe YS, Chi DY, Kim B-T. Radiolabeled RGD Uptake and Alphav Integrin Expression Is Enhanced in Ischemic Murine Hindlimbs. J Nucl Med. 2005; 46(3):472–478. [PubMed: 15750161]

33. Lu E, Wagner WR, Schellenberger U, Abraham JA, Klibanov AL, Woulfe SR, Csikari MM, Fischer D, Schreiner GF, Brandenburger GH, et al. Targeted in Vivo Labeling of Receptors for Vascular Endothelial Growth Factor: Approach to Identification of Ischemic Tissue. Circulation. 2003; 108(1):97–103. [PubMed: 12821549]

34. Willmann JK, Chen K, Wang H, Paulmurugan R, Rollins M, Cai W, Wang DS, Chen IY, Gheysens O, Rodriguez-Porcel M, et al. Monitoring of the Biological Response to Murine Hindlimb Ischemia with 64Cu-Labeled Vascular Endothelial Growth Factor-121 Positron Emission Tomography. Circulation. 2008; 117(7):915–922. [PubMed: 18250264]

35. Dallas NA, Samuel S, Xia L, Fan F, Gray MJ, Lim SJ, Ellis LM. Endoglin (CD105): A Marker of Tumor Vasculature and Potential Target for Therapy. Clin Cancer Res. 2008; 14(7):1931–1937. [PubMed: 18381930]

36. Tu T, Zhang C, Yan H, Luo Y, Kong R, Wen P, Ye Z, Chen J, Feng J, Liu F, et al. CD146 Acts as a Novel Receptor for Netrin-1 in Promoting Angiogenesis and Vascular Development. Cell Res. 2015; 25:275. [PubMed: 25656845]

37. Jiang T, Zhuang J, Duan H, Luo Y, Zeng Q, Fan K, Yan H, Lu D, Ye Z, Hao J, et al. CD146 Is a Coreceptor for VEGFR-2 in Tumor Angiogenesis. Blood. 2012; 120(11):2330 LP–2339. [PubMed: 22718841]

38. Zeng Q, Wu Z, Duan H, Jiang X, Tu T, Lu D, Luo Y, Wang P, Song L, Feng J, et al. Impaired Tumor Angiogenesis and VEGF-Induced Pathway in Endothelial CD146 Knockout Mice. Protein Cell. 2014; 5(6):445–456. [PubMed: 24756564]

39. Tirziu D, Moodie KL, Zhuang ZW, Singer K, Helisch A, Dunn JF, Li W, Singh J, Simons M. Delayed Arteriogenesis in Hypercholesterolemic Mice. Circulation. 2005; 112(16):2501–2509. [PubMed: 16230502]

40. Helisch A, Wagner S, Khan N, Drinane M, Wolfram S, Heil M, Ziegelhoeffer T, Brandt U, Pearlman JD, Swartz HM, et al. Impact of Mouse Strain Differences in Innate Hindlimb Collateral Vasculature. Arterioscler Thromb Vasc Biol. 2006; 26(3):520–526. [PubMed: 16397137]

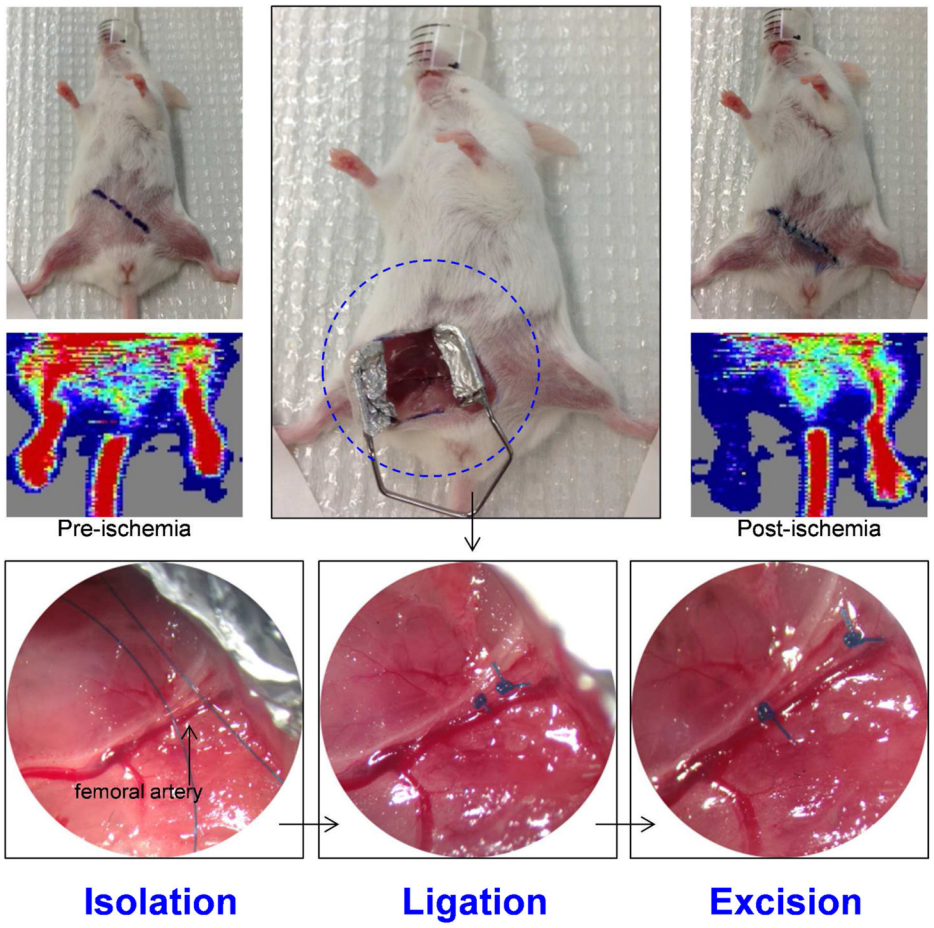

Figure 1.

Representative images of the hindlimb ischemia model generation, showing the step-by-step process of the surgical procedure that includes the isolation of the femoral artery, its ligation at the proximal and distal sites followed by its complete excision. Laser Doppler images acquired before and after the induction of ischemia corroborates the reduced blood flow in the operated leg.

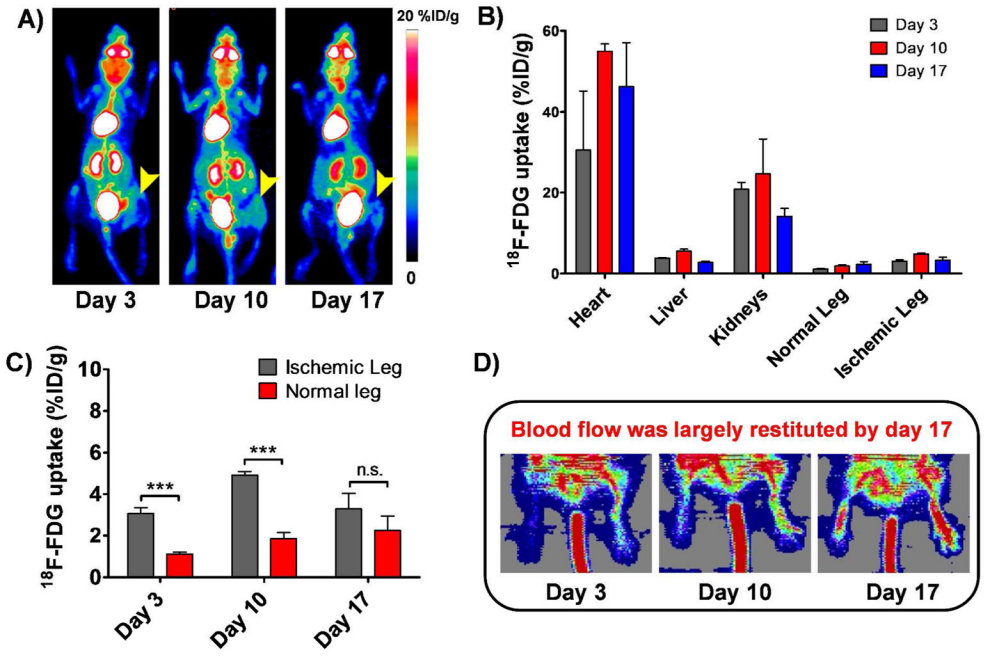

Figure 2.

A) Serial maximum intensity projection (MIP) PET images of mice injected with ^{18}F-FDG on postoperative days 3, 10 and 17. Arrowhead points to the ischemic leg. Tracer uptake in the ischemic leg, despite being significantly higher in the ischemic leg, was still considered to be low. **B)** PET imaging-derived ^{18}F-FDG uptake, reported as %ID/g ± SD, in different tissues on postoperative days 3, 10 and 17 (n=3). **C)** Comparative graph showing ^{18}F-FDG uptake in the ischemic and non-operated legs on postoperative days 3, 10 and 17. **D)** Serial Laser Doppler imaging of non-ischemic (right side) and ischemic hindlimbs (left side) of balb/c mice undergone surgery. Dark blue areas, observed at day 3, indicate decreased perfusion in the injured limb, while high perfusion pattern (red color) is observed in the contralateral hindlimb. Some perfusion recovery was detectable by day 10 and blood flow was largely restituted in the operated hindlimb by day 17.

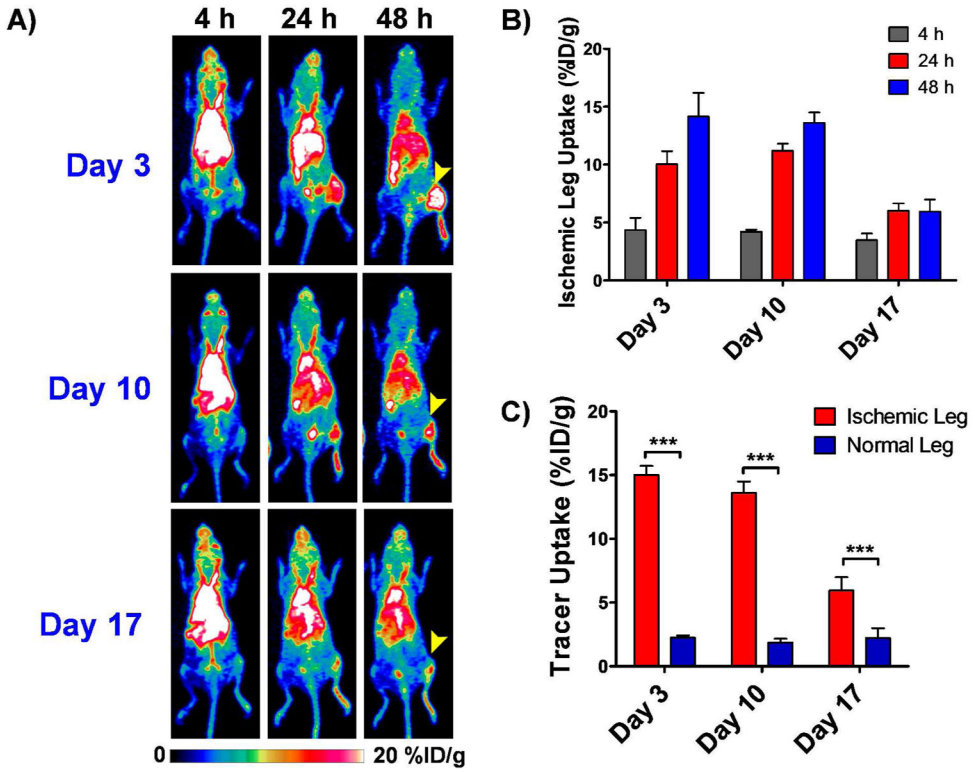

Figure 3.

Longitudinal PET imaging studies in ischemic mice injected intravenously with 5–10MBq (135–270 μCi) of ^{64}Cu-NOTA-YY146 on postoperative days 3, 10 and 17. **A)** Serial maximum intensity projection (MIP) PET images at 4, 24 and 48h p.i. at the different postoperative timepoints. Arrow heads point to the ischemic leg. **B)** Tracer uptake, represented as mean %ID/g ± SD, in the ischemic leg at different time points on the different postoperative days. **C)** Comparative graph showing peak tracer uptake in the ischemic and non ischemic legs at 48h p.i. on postoperative days 3, 10 and 17.

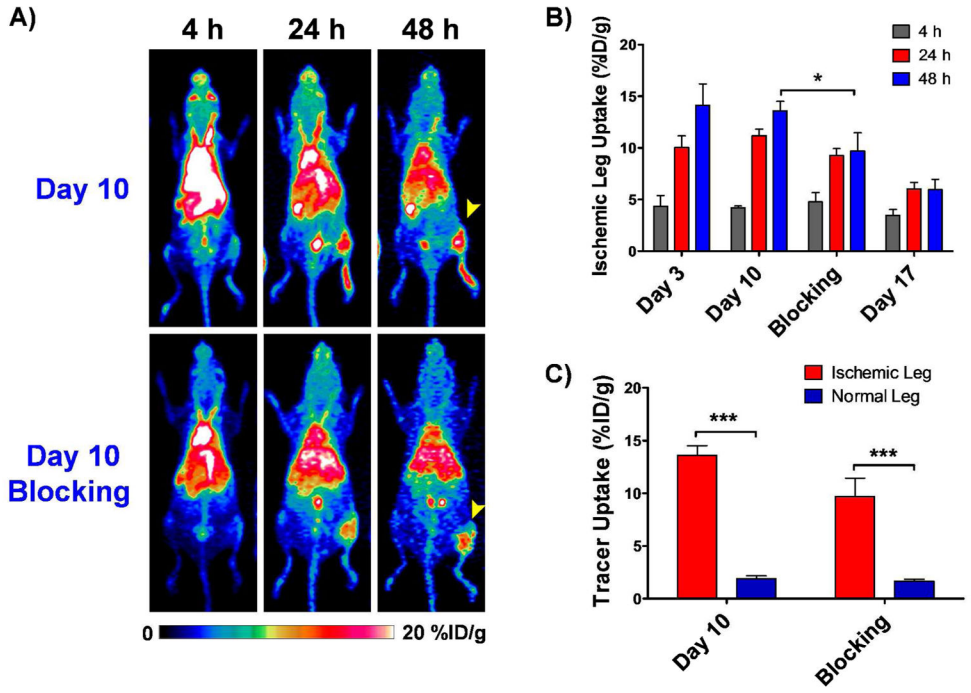

Figure 4.

Results from the Blocking Study carried out on a postoperative day 10. Arrowhead points to the ischemic leg. **A)** Serial maximum intensity projection (MIP) PET images at 4, 24 and 48h p.i on day 10 of mice with and without pre-injection of blocking dose. **B)** Tracer uptake, represented at %ID/g, in the ischemic leg at different time points on different postoperative days, including the blocking group on day 10. Error bars represent standard deviation. **C)** Comparative graph showing tracer uptake in the injured and non ischemic legs at 48h p.i. on postoperative day 10 with and without pre-injection of blocking dose.

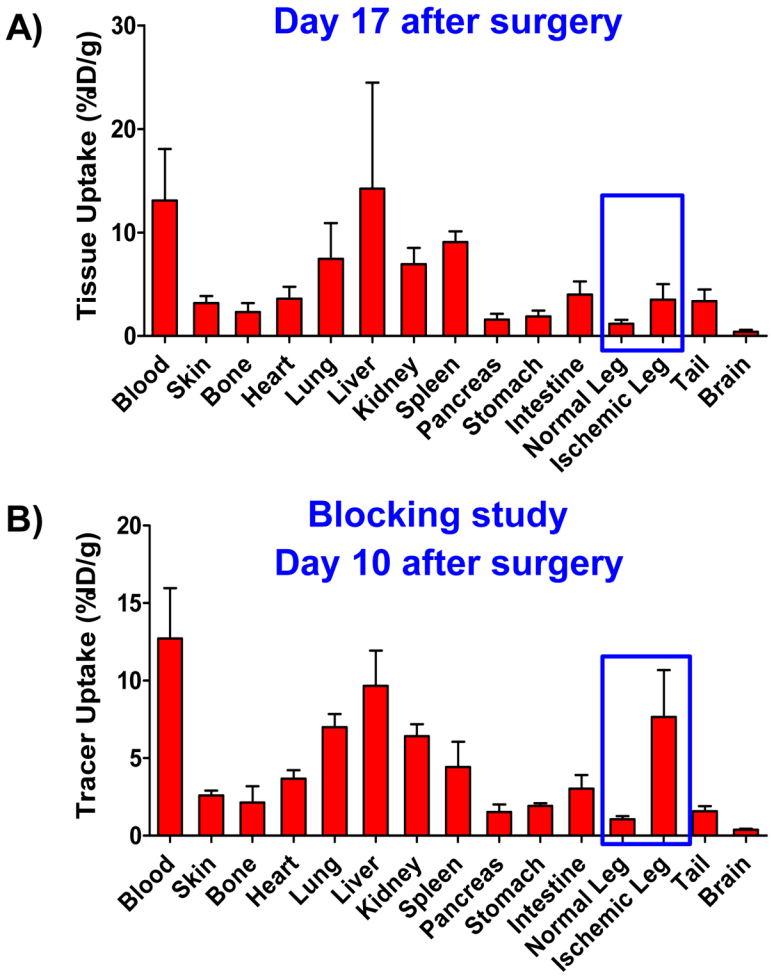

Figure 5.

Ex vivo^{64} Cu-NOTA-YY146 biodistribution data obtained right after the last PET scan (48h p.i.) at **A)** postoperative day 17 and **B)** postoperative day 10. In blocking studies, mice were administered a blocking dose (10 mg/kg) of cold YY146 24 hours before the radiolabeled tracer was intravenously injected. Animals were sacrificed, and tissue samples were harvested, wet-weighed, gamma counted, and tracer uptake in the different tissues was calculated as %ID/g (mean ± SD).

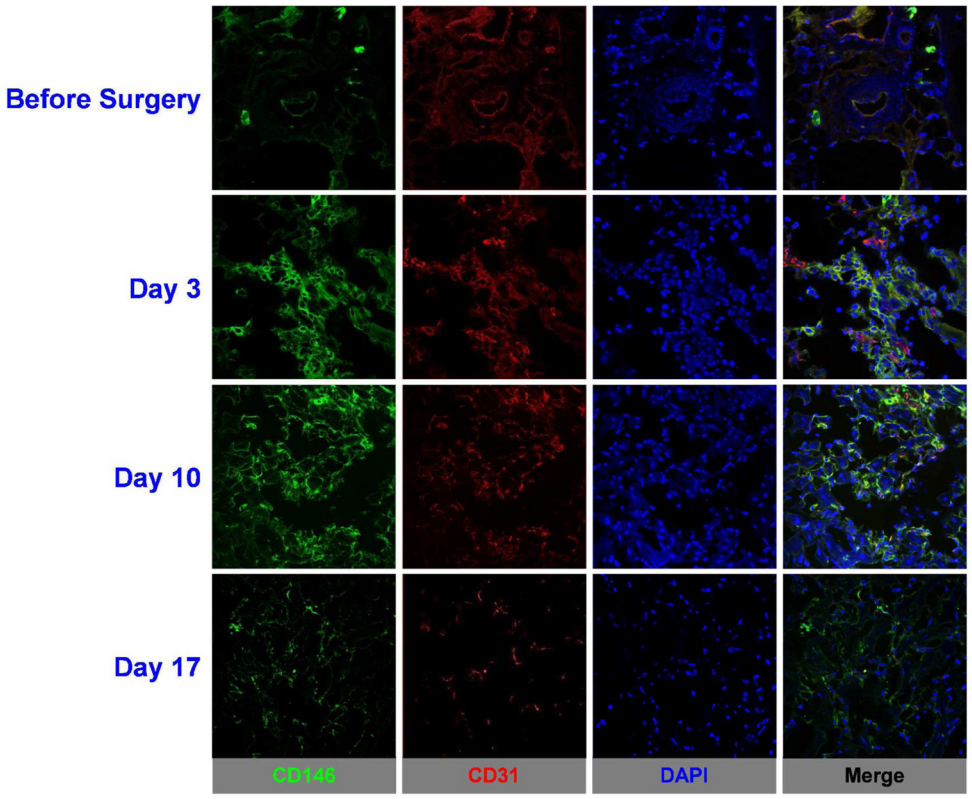

Figure 6.

Immunofluorescence staining demonstrated increased CD146 expression in the ischemic muscle tissue on postoperative days 3 and 10, but marginal, background levels at day 17, indicating a return to a normal expression pattern. Green: CD146; red: CD31; blue: DAPI. Scale bar = 50μm. AUTHOR INFORMATION